CONF-910869--13

DE92 000048

FULL-WAVE CALCULATION OF FAST-WAVE CURRENT DRIVE IN TOKAMAKS INCLUDING $k_{\|}$ UPSHIFTS*

E. F. Jaeger and D. B. Batchelor

Oak Ridge National Laboratory, Oak Ridge, TN 37831-8071

INTRODUCTION

Numerical calculations of fast-wave current drive (FWCD) efficiency have generally been of two types: ray tracing or global wave calculations. Ray tracing shows that the projection of the wave number ($k_{\|}$) along the magnetic field can vary greatly over a ray trajectory, particularly when the launch point is above or below the equatorial plane.[1] This variation is caused predominantly by the poloidal magnetic field in a tokamak. As the wave penetrates toward the center of the plasma, $k_{\|}$ increases, causing a decrease in the parallel phase speed ($\mathrm{w} = v_{\mathrm{phase}}/v_{\mathrm{th}} = \omega/k_{\|}v_{\mathrm{th}}$) and a corresponding decrease in the current drive efficiency, γ. But the assumptions of geometrical optics, namely short wavelength and strong single-pass absorption, are not generally applicable in FWCD scenarios. Eigenmode structure, which is ignored in ray tracing, can play an important role in determining electric field strength and Landau damping rates. In such cases, a full-wave or global solution for the wave fields is desirable.

In full-wave calculations such as ORION[1,2] which use finite differencing in the poloidal dimension, $k_{\|}$ appears as a differential operator ($\vec{B}\cdot\nabla$) in the argument of the plasma dispersion function. Since this leads to a differential system of infinite order, such codes of necessity assume $k_{\|} \sim k_{\varphi} = \mathrm{const}$, where k_{φ} is the toroidal wave number. Thus, it is not possible to correctly include effects of the poloidal magnetic field on $k_{\|}$. The problem can be alleviated by expressing the electric field as a superposition of poloidal modes,[3] in which case $k_{\|}$ is purely algebraic. This paper describes a new full-wave calculation, PICES (Poloidal Ion Cyclotron Expansion Solution), which uses poloidal and toroidal mode expansions to solve the wave equation in general flux coordinates. The calculation includes a full (nonperturbative) solution for $E_{\|}$ and uses a reduced-order form of the plasma conductivity tensor[4] to eliminate numerical problems associated with resolution of the very short wavelength ion Bernstein wave.[3]

Although the expansion in poloidal modes allows a more accurate calculation of electron heating, it is difficult to separate this power deposition according to resonant parallel velocity and poloidal position on a flux surface, and therefore to calculate driven current. Here we suggest a method to make this separation, and apply the model to current drive scenarios in the ITER and DIII-D tokamaks.

* Research sponsored by the Office of Fusion Energy, U.S. Department of Energy, under contract DE-AC05-84OR21400 with Martin Marietta Energy Systems, Inc.

DISCLAIMER

PICES NUMERICAL TECHNIQUE

The computer code PICES calculates three components of the ICRF wave electric field (E_ψ, E_η, E_b) and the power absorbed per unit length $\left[\dot{W} = \frac{1}{2}\mathrm{Re}(\vec{E}^* \cdot \vec{J}_p)\right]$ by solving the reduced-order wave equation in two spatial dimensions (ρ, ϑ). A poloidal mode expansion in ϑ allows the variation in $k_\parallel$ to be included rigorously, while the ρ dimension is treated by finite differences. Variations in the toroidal dimension (ζ) are calculated by summing toroidal harmonics weighted by a particular antenna spectrum. Toroidal harmonics are uncoupled due to symmetry in tokamak geometry and can thus be calculated individually. Poloidal modes, on the other hand, are tightly coupled by the toroidal $(1/R)$ dependence of $\vec{B}$ and must therefore be calculated simultaneously. This is accomplished by direct matrix inversion of the finite-difference equations for all poloidal modes simultaneously.

FAST-WAVE CURRENT DRIVE

The current density $J_\parallel(\rho, \vartheta)$ which is driven by fast waves is directly proportional to the power absorbed by the electrons $\dot{W}_e$:

$$J_\parallel(\rho, \vartheta) = C_E\left(\rho, \vartheta, k_\parallel\right) \dot{W}_e(\rho, \vartheta). \tag{1}$$

Ehst[5] has provided an algebraic expression for $C_E\left(\rho, \vartheta, k_\parallel\right)$ from the Fokker-Planck results of Karney.[6] In Eq. (1), $k_\parallel$ is the local value in space, $k_\parallel(\rho, \vartheta)$. For one such local value $k_\parallel(\rho, \vartheta) = k_\parallel^0$ we must sum over all poloidal and toroidal harmonics m, n which give $k_\parallel^0$ when calculating $\dot{W}_e$. Then all values of $k_\parallel^0$ must be summed. For a single value of n corresponding to an antenna spectrum which is a δ-function in k_φ, this gives

$$J_\parallel(\rho, \vartheta) = \sum_m C_E\left(\rho, \vartheta, k_\parallel^m\right) \frac{1}{2} Re\left[\vec{E}_m^* \cdot \vec{\vec{\sigma}}\left(\rho, \vartheta, k_\parallel^m\right) \vec{E}_m\right], \tag{2}$$

which corresponds to dropping the cross terms in $\dot{W}_e(\rho, \vartheta)$. This is not unreasonable since $C_E\left(\rho, \vartheta, k_\parallel^m\right)$ is a slowly varying function of ϑ and the cross terms average approximately to zero in the WKB sense when $J_\parallel(\rho, \vartheta)$ is averaged over a flux surface.

EFFECT OF $k_\parallel$ UPSHIFT IN ITER

We consider the low-frequency FWCD scenario for ITER.[7] Parameters are consistent with ITER in the "steady-state, technology phase," i.e., $R_0 = 6.0$ m, $B_0 = 4.8$ T, $f = 17$ MHz, $a_{\mathrm{plasma}} = 2.15$ m, $a_{\mathrm{wall}} = 2.3$ m, $K = 2.0$, $T_e(0) = T_i(0) = 33$ keV, $\langle T_e \rangle = \langle T_i \rangle = 20$ keV, $n_{e0} = 1.1 \times 10^{20}$ m^{-3}, $\langle n_e \rangle = 0.7 \times 10^{20}$ m^{-3} with a 50-50 mixture of D-T gas and $Z_{\mathrm{eff}} = 2.26$.

Density and temperature profiles are parabolas raised to the α_n and α_T powers respectively, with $\alpha_n = 0.5$ and $\alpha_T = 1.0$.

Figure 1 shows contours of electron power absorption $\dot{W}_e(\rho, \vartheta)$ due to Landau damping and transit time magnetic pumping (TTMP) for an antenna centered on the midplane and $k_\varphi = 0.8333$ m^{-1} ($n_\varphi = -5$) and $q_0 = 1.0$ in a Solov'ev equilibrium. Figures 1(a) and (b) show, respectively, results with and without the shift in $k_\parallel$. Clearly the effect of the $k_\parallel$ shift in Fig. 1(a) is to allow more heating and wave damping in the outer regions of the plasma, where current drive efficiency is the lowest due to trapped particle effects. This results in a flux-surface-average current profile in Fig. 2 (solid) which is narrower with a lower efficiency $\gamma = 0.20$ A/W-m^2 than the corresponding result for $k_\parallel = k_\varphi$ (dashed) with $\gamma = 0.312$ A/W-m^2. The dashed curve and efficiency agree with previous ORION results.[1] Optimizing γ with respect to toroidal mode number n_φ gives the highest efficiency $\gamma \sim 0.2$ A/W-m^2 at $n_\varphi = -4$ for $q_0 = 1.0$ and $\gamma \sim 0.364$ A/W-m^2 at $n_\varphi = -3$ for $q_0 = 2.0$. The strong sensitivity with respect to safety factor q is to be expected since the $k_\parallel$ upshift is caused predominantly by the poloidal field in ITER. Since the q profile in the Solov'ev equilibrium is relatively flatter than in a real tokamak, $q_0 = 2.0$ may give a more accurate representation of the upshift than $q_0 = 1.0$. More realistic results of course require a better calculation for the tokamak equilibrium. Ray tracing results[8,1] for this case give γ in the range 0.25 to 0.39 for toroidal mode numbers $4 \leq n_\varphi \leq 7$. Complete agreement between ray tracing and full-wave results is not to be expected here since single-pass absorption is only about 27% in this case, and wall reflections with the resulting cavity modes are clearly important. These results suggest that when single-pass absorption is not complete, the remaining reflected power drives current nearly as effectively as the power absorbed on the first pass.

FWCD IN THE DIII-D TOKAMAK

Next we consider three possible scenarios for FWCD experiments which are just beginning on the DIII-D tokamak. For these calculations we use parameters consistent with projections for these experiments, i.e., $R_0 = 1.67$ m, $B_0 = 1.0$ T, $f = 60$ MHz, $a_{\text{plasma}} = 0.63$ m, $a_{\text{wall}} = 0.72$ m, $K = 1.8$, $T_e(0) = 4$ keV, $T_i(0) = 3$ keV, $n_{e0} = 2.0 \times 10^{19}$ m^{-3}, $\langle n_e \rangle = 1.33 \times 10^{19}$ m^{-3} in pure D_2 gas with $Z_{\text{eff}} = 1.5$. Profiles are calculated with $\alpha_n = 0.5$ and $\alpha_T = 5.0$, giving very peaked temperature profiles. Figure 3(a) shows the FWCD efficiency γ as a function of electron temperature for three cases: (1) $k_\varphi \sim 7$ m^{-1} and $f = 60$ MHz (solid circles); (2) $k_\varphi \sim -7$ m^{-1} and $f = 120$ MHz (open circles) and (3) $k_\varphi \sim -5$ m^{-1} and $f = 60$ MHz (open triangles). The solid line in Fig. 3(a) assumes w = 2.0. The corresponding power absorption is shown in Fig. 3(b) for each case. The dashed curve is the normalized analytic expression[9] for electron power absorption due to combined electron Landau damping (ELD) and TTMP for $k_\varphi \sim -7$ m^{-1} and $f = 60$ MHz.

The solid circles in Fig. 3 can be associated with the present four-strap antenna design in the idealized case that $\pi/2$ phasing gives a perfect δ-function spectrum at $k_\varphi \sim -7$ m^{-1} ($2\pi/4 \times$ strap spacing). Of course the actual spectrum

will be much more complicated than this, but the simple calculation for a single value of k_φ can give some insight into efficiency of power absorption and current drive. For example, when the frequency is increased to 120 MHz (open circles) for the same value of k_φ, the current drive efficiency improves since particle trapping is less. The waves, however, are too fast to couple efficiently to thermal electrons and power absorption suffers dramatically. Alternatively, by modifying the phasing at 60 MHz so that $k_\varphi \sim -5\ \mathrm{m}^{-1}$ (open triangles), the efficiency can be made comparable to that at 120 MHz while maintaining good absorption. This result is similar to what can be obtained with $f = 120$ MHz and $k_\varphi \sim -10\ \mathrm{m}^{-1}$ (the dominant mode for a six-strap antenna at $\pi/2$ phasing and 120 MHz).

SUMMARY AND CONCLUSIONS

We have seen that as waves propagate toward the center of a tokamak, the $k_\parallel$ spectrum excited at the plasma edge by the antenna is not maintained but can shift due to the presence of the finite poloidal field. This shift can have a very important influence on wave damping and current drive. It has not been possible to accurately model this effect in global-wave calculations such as ORION[1,2] which use finite differencing in the poloidal dimension because $k_\parallel$ appears as a differential operator in the argument of the plasma dispersion function. This problem has been dealt with in PICES, a new full-wave calculation which represents the wave fields as a superposition of toroidal and poloidal modes, in which case $k_\parallel$ reduces to an algebraic operator. A simplified current drive model separates power deposition according to resonant parallel velocity and poloidal position on a flux surface. In cases for which the single-pass absorption is large, the current drive efficiency agrees with ray tracing. When single-pass absorption is low, the reflected power drives current nearly as efficiently as that absorbed on the first pass. To get an accurate result, one must of course calculate the complete antenna k_φ spectrum, not simply use the peak value as was done here.

REFERENCES

1. D. B. Batchelor et al., in Proceedings of the 13th International Conference on Plasma Physics and Controlled Nuclear Fusion Research, Washington, 1990 (IAEA, Vienna, in press), IAEA-CN-53/E-3-11.
2. E. F. Jaeger, D. B. Batchelor, M. D. Carter, and H. Weitzner, Nucl. Fusion **30**, 505 (1990).
3. M. Brambilla and T. Krucken, Nucl. Fusion **28**, 1813 (1988).
4. D. N. Smithe, P. L. Colestock, R. J. Kashuba, and T. Kammash, Nucl. Fusion **27**, 1319 (1987).
5. D. A. Ehst and K. Evans, Jr., Nucl. Fusion **27**, 1267 (1987).
6. C. F. F. Karney and N. J. Fisch, Phys. Fluids **28**, 116 (1985).
7. J. Jacquinot. private communication (March 9, 1990).
8. V. Bhatnagar, private communication (June 6, 1990).
9. P. E. Moroz and P. L. Colestock, Plasma Phys. Controlled Fusion **33**, 417 (1991).

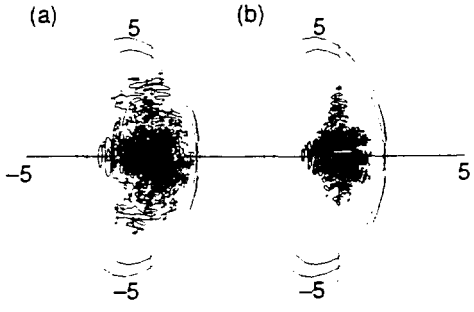

Fig. 1. Contours of electron power absorption in ITER (a) including $k_{\|}$ variations and (b) with $k_{\|} = k_{\varphi}$.

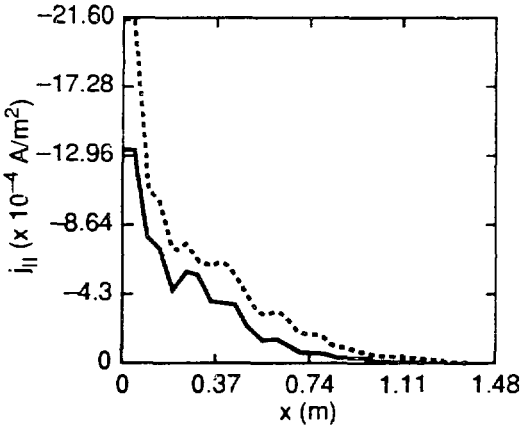

Fig. 2. Flux surface average of the driven current density in ITER with $k_{\|}$ variations included (solid) and with $k_{\|} \sim k_{\varphi}$ (dashed).

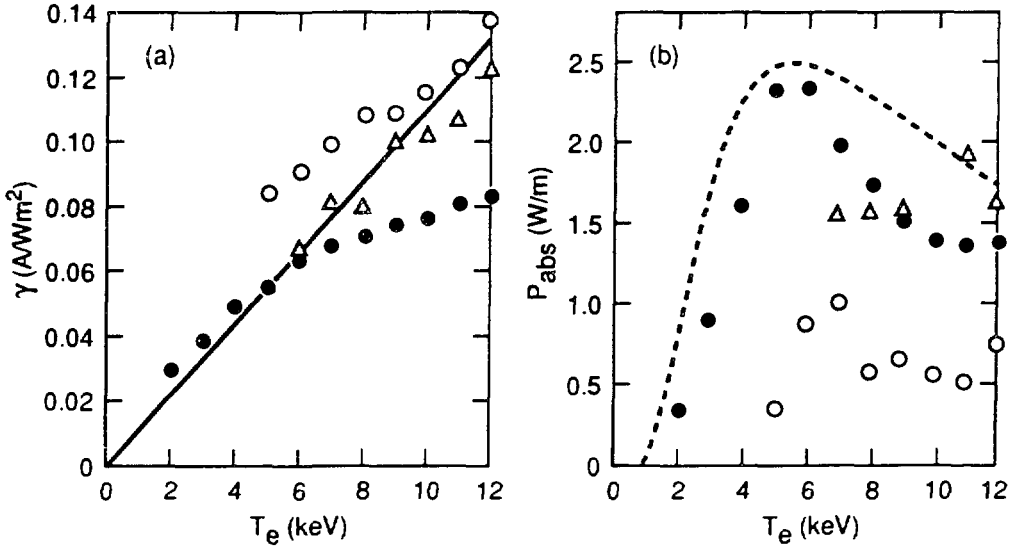

Fig. 3. (a) Current drive efficiency γ and (b) power absorption vs electron temperature for three scenarios in DIII-D: (1) k_{φ} - 7 m^{-1} and f 60 MHz (solid circles); (2) k_{φ} -- 7 m^{-1} and f 120 MHz (open circles); and (3) k_{φ} -- -5 m^{-1} and f = 60 MHz (open triangles).